Imaging Systems and Audio Control Utilizing Acoustics

Siti Nur Nasha Azlika Hamidon[1], Siti Zaleha Abdul Hamid[1], Herlina Abdul Rahim[1*], Nur Athirah Syafiqh Noramli[2]

[1*] Faculty of Electrical Engineering, Universiti Teknologi Malaysia, 81310 Skudai, Johor, Malaysia
[2] School of Electrical Engineering, College of Engineering, Universiti Teknologi MARA, Shah Alam, Selangor. Malaysia

Corresponding author* email: herlina@utm.my
Available online 30 June 2024

ABSTRACT

Conventional noise reduction materials such as concrete, wood, foam, and glass are widely used in buildings to minimize environmental noise. However, these materials have limited effectiveness in reducing low-frequency noise. Acoustic metamaterials have been introduced as a more efficient alternative, offering superior low-frequency sound reduction while being lighter and more cost-effective than traditional bulky materials. This study investigates the feasibility of acoustic metamaterials for noise reduction. Five acoustic enclosure samples were fabricated using different materials, each with dimensions of 100 mm³. The wood enclosure was manually constructed, while acrylonitrile butadiene styrene (ABS), polylactic acid (PLA), PLA with a 1 mm-thick metamaterial layer, and PLA with a 5 mm-thick metamaterial layer were produced using three-dimensional (3D) printing. The performance of these enclosures was evaluated based on the decibel (dB) drop, measuring the difference in sound pressure levels before and after placing the enclosure over the sound source. Among all samples, the PLA enclosure with a 5 mm-thick metamaterial layer demonstrated the highest noise reduction, achieving a maximum sound pressure level reduction of 26.1 dB at 800 Hz. This result confirms that increasing the metamaterial thickness enhances sound reduction performance.

Keywords: Sound Reduction, Noise Reduction, Acoustic Metamaterials, Metamaterials, Acoustic Enclosure.

1. Introduction

Noise pollution is a common issue in major cities such as Tokyo, Sydney, and London. In these urban areas, heavy road traffic is a significant source of noise pollution, whereas in developing countries like Malaysia, construction activities are the predominant contributors [1]. Noise pollution consists of both high-frequency and low-frequency noise sources.

To mitigate noise pollution, noise-reducing materials have been incorporated into buildings, bridges, cooling towers, and heavy industrial areas as an alternative solution [2]. Conventional noise reduction materials, such as concrete, wood, foam, and glass, are widely used in buildings to minimize environmental noise. However, these materials are not effective in reducing low-frequency noise [3] due to the longer wavelengths associated with these frequencies [4]. Traditional low-frequency noise-reducing materials, such as concrete and wood, tend to be heavy and expensive [5].

Technological advancements in acoustic engineering have led to the development of metamaterials, which offer superior low-frequency noise reduction while being lighter and more cost-effective than conventional bulky materials [6]. This study aims to investigate the feasibility of acoustic metamaterials for noise reduction.

Acoustic waves are longitudinal waves characterized by variations in pressure and particle velocity, which are essential parameters for wave description [7],[8]. Metamaterials function by replacing the molecular structure of conventional materials with engineered structures on a scale significantly smaller than the target wavelength, enabling enhanced noise reduction capabilities [9].

1.1 Acoustic Matematerial Properties

Acoustic metamaterials utilize the precisely engineered motion of their small-scale structures to achieve extraordinary acoustic properties that are absent in conventional materials derived from natural sources.

Porous acoustic metamaterials consist of stacked perforated plates made from acoustically rigid materials, separated by a sound-supporting fluid such as air. This design allows sound waves to propagate through the metamaterial. The primary component of this structure is a hole array, which enables sub-wavelength control over sound wave transmission. Unlike sonic crystals, porous metamaterials do not rely on diffraction to achieve negative refraction [7].

In resonant-structured acoustic metamaterials, a limited frequency range is achieved by uniformly distributing small metallic elements within the air, forming sonic crystals. These sonic crystals function as sound absorbers on their own, with their arrangement and design influencing their extreme acoustic properties [7]. Additionally, the peak sound absorption coefficient shifts to lower frequencies as the air layer thickness increases.

To enhance low-frequency sound absorption, both porous [7] and resonant [10],[11] structures are integrated into acoustic metamaterials [12],[13]. The combination of porous structures [14] and Helmholtz resonator (HR) geometrical characteristics creates resonating cavities, slowing down the propagation of sound waves through the metamaterials [15]. This design enables acoustic metamaterials to effectively control and manipulate sound waves, regardless of the incident angle upon the surface.

1.2 Unit Cell Metamaterial Design

A unit cell of the metamaterial was designed using the wavelength equation and the Helmholtz resonator (HR) concept to determine appropriate measurements and structural design. The primary requirement for this configuration is the presence of a resonance condition [16],[17].

The fundamental wavelength equation is presented in (1), where λ represents the wavelength of sound waves, v is the speed of sound in air, and f is the frequency of the sound waves. For optimal sound absorption, the material thickness must align with the wavelength corresponding to the target frequency.

The frequency of the Helmholtz resonator, fH, is determined using equation (2), where c denotes the speed of sound, $Aneck$ is the cross-sectional area of the neck, $Vcavity$ is the volume of the cavity, and heq represents the equivalent height of the neck.

$$\lambda = v / f(m) \tag{1}$$

$$f_H = \frac{c}{2\pi} \times \sqrt{\frac{A_{neck}}{V_{cavity} h_{eq}}} \tag{2}$$

As defined in equations (3), (4), and (5), the parameters $Vneck$ (neck volume), $hneck$ (neck height), D (neck diameter), $lneck$ (neck length), and $wneck$ (neck width) are established. Similarly, assuming equations (6), (7), and (8), the cavity parameters $lcavity$ (length), $hcavity$ (height), and $wcavity$ (width) are defined. Consequently, $Aneck$ and $Vcavity$ are derived as shown in equations (9) and (10), respectively.

$$A_{neck} = \frac{V_{neck}}{h_{eq}} \tag{3}$$

$$h_{eq} = h_{neck} + 0.3D \tag{4}$$

$$D = \frac{2 l_{neck} w_{neck}}{l_{neck} + w_{neck}} \tag{5}$$

$$l_{neck} = \frac{1}{3} l_{cavity} \tag{6}$$

$$h_{neck} = \frac{1}{6} h_{cavity} \tag{7}$$

$$w_{neck} = \frac{1}{2} w_{cavity} \tag{8}$$

$$A_{neck} = l_{neck} \times h_{neck} \tag{9}$$

$$V_{cavity} = l_{cavity} \times w_{cavity} \times h_{cavity} \tag{10}$$

1.3 Performance Analysis

The performance analysis of the acoustic enclosure samples was evaluated based on the decibel drop (**d**), which indicates the difference in sound pressure levels before and after placing the acoustic enclosure over the sound source. The decibel drop can be determined using equation (11), where **dBsource** represents the sound pressure level before the enclosure is applied, and **dBmaterials** represents the sound pressure level after the enclosure is in place.

$$d = dB_{source} - dB_{materials} \tag{11}$$

2. Methodology

The development of acoustic metamaterials consisted of four stages, which are parametric study of acoustic metamaterials unit cell design, acoustic metamaterial simulation, fabrication of acoustic enclosure samples, and experimental testing in sound reduction.

2.1 Metamaterial Unit Cell Design

The design of acoustic metamaterials was conducted within a frequency range of 200 Hz to 1000 Hz. Initially, the wavelengths corresponding to the minimum and maximum frequencies were determined using the fundamental wavelength equation (1). At room temperature, where the speed of sound is 343.2 m/s, the calculated wavelengths for 200 Hz (**λ200**) and 1000 Hz (**λ1000**) are 1.7160 m and 0.3432 m, respectively. The longer wavelength at 200 Hz is attributed to its lower frequency characteristics.

A crucial aspect of metamaterial design is determining subwavelength thickness based on wave propagation through the material. Since metamaterials must have a thickness significantly smaller than the wavelength of the sound waves they interact with, the thickness should be much less than 1.716 m, which represents the maximum thickness. To facilitate fabrication and experimental testing, millimeters (mm) were selected as the unit of measurement. The resonant frequency, at which peak absorption occurs, corresponds to one-quarter of the incident sound wavelength and is calculated using equations (12) and (13).

$$\lambda_{resonant} = \frac{1}{4} \times Thickness\max = \frac{1}{4} \times 1.716 = 0.429\,m \tag{12}$$

$$f_{resonant} = \frac{v}{\lambda_{resonant}} = \frac{343.2}{0.429} = 800Hz \tag{13}$$

Table 1. Parameter Scale in Metamaterial Design with HR

Parameter	Scale
Length of cavity, l_{cavity}	3mm
Height of cavity, h_{cavity}	6cm
Width of cavity, w_{cavity}	20mm
Length of neck, l_{neck}	1mm
Height of neck, h_{neck}	1cm
Width of neck, w_{neck}	10mm
Diameter of neck, D	1.8182×10^{-3}
Equivalent height of neck, h_{eq}	0.01055m
Area of neck, A_{neck}	$1 \times 10^{-5} m^2$
Volume of cavity, V_{cavity}	$3.6 \times 10^{-6} m^2$
Frequency of HR, f_H	886.32Hz

The dimensions of the area and volume of the Helmholtz resonator (HR) were calculated. The obtained parameters were compiled and presented in Table 1. The unit cell was designed using the 3D modeling software TinkerCAD. The key factors ensuring resonance in this design were the presence of an opening on the neck, the neck's cross-sectional area, and the cavity's volume.

In the design, unit cells were arranged side by side with a 0.5 mm gap between them and grouped into a row of six unit cells. A cube-shaped acoustic enclosure with dimensions of 100 mm³ was then constructed, featuring a surface

thickness (**t**) of 5 mm, as illustrated in Figure 1. The grouped unit cells were positioned on each inner wall of the enclosure. While there is no fixed limit on the number of unit cells per wall, increasing the number requires greater fabrication precision. A parametric study was conducted to determine the optimal number of unit cells for fabrication on each wall.

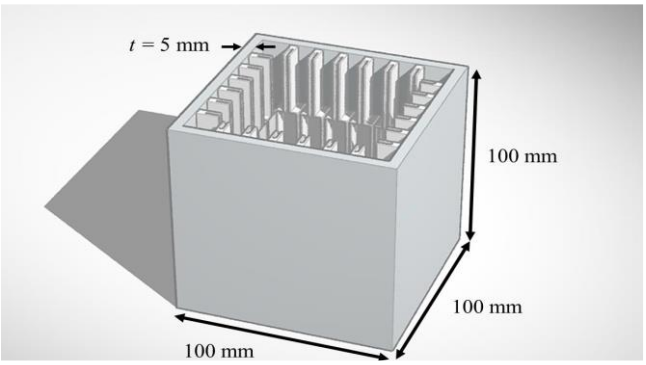

Figure 1. 3D Acoustic Metamaterial Designed

2.2 Unit Cell Design Simulation

The unit cell was simulated in COMSOL Multiphysics using the eigenfrequency module, with boundaries assumed to be hard and rigid. The study focused on analyzing acoustic pressure (AP) and sound pressure level (SPL) for frequencies below 1000 Hz. The primary objective of this simulation was to determine the eigenfrequency of the unit cell and ensure that it falls outside the 200–1000 Hz range. This precaution prevents unwanted vibrations caused by sound waves interacting with the metamaterial. If the eigenfrequency falls within this range, the unit cell design must be modified until it is below the specified threshold.

Before starting the simulation, ensure that the module is set to .acpr by selecting "Pressure Acoustics" in the frequency domain. The geometry should be placed on the work plane, with the surrounding medium defined as air. The material properties are specified with a density of 1.25 kg/m³ and a sound speed of 343 m/s. A mesh is then generated to validate the boundaries and domains for the eigenfrequency study. Finally, the eigenfrequency simulation is conducted with a frequency setting of 1000 Hz to obtain eigenfrequencies near this value.

2.3 Fabrication of Acoustic Enclosure

Five acoustic enclosure samples were fabricated using different materials, each with dimensions of 100 mm³. The wood-based acoustic enclosure was manually constructed, while enclosures made of acrylonitrile butadiene styrene (ABS), polylactic acid (PLA), PLA with metamaterial (1 mm thickness), and PLA with metamaterial (5 mm thickness) were digitally fabricated using three-dimensional (3D) printing.

The manually fabricated wooden acoustic enclosure, shown in Figure 2, was assembled from five wood panels, each measuring 100 mm², which were cut and joined using acoustic sealant. The outer surface was sanded to ensure a smooth finish for safe handling during experiments. Proper safety precautions, including the use of gloves, goggles, and masks, were followed throughout the fabrication process.

For digital fabrication, the 3D printing setup for the acoustic enclosure is illustrated in Figure 3. The design file (.stl format) was first imported from 3D modeling software before printing with a FlashForge Dreamer 3D printer. Prior to printing, the filament was correctly loaded into the extruder, and both the filament and platform were preheated while ensuring the platform was clean. During printing, the printer cover was securely placed to maintain a stable internal temperature, preventing distortions in the printed sample. Once the printing process was complete, the platform was preheated again, and the printed sample was carefully removed.

The final 3D-printed acoustic enclosures, including the standard acoustic enclosure and the metamaterial-integrated enclosure, are displayed in Figure 4 (a) and (b), respectively.

Figure 2. Wood Acoustic Enclosure with Dimension of 100 mm^3

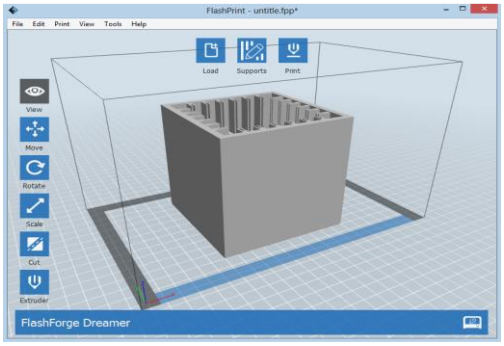

Figure 3. 3D Design of Acoustic Enclosure Printing Setup

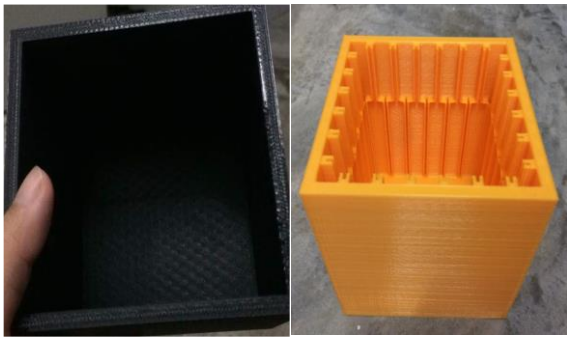

(a) (b)

Figure 4. 3D Printed of (a) Acoustic Enclosure and (b) Acoustic Enclosure with Metamaterial

2.4 Sound Reduction Experiment

The acoustic enclosure samples were tested for sound reduction across frequencies ranging from 200 to 1000 Hz. This experiment was conducted to evaluate the effectiveness of each enclosure in reducing sound levels.

The experimental setup, illustrated in Figure 5, included a sound level meter to measure the sound pressure level (SPL) in a controlled room environment. A wireless speaker served as the sound source, generating pure tones between 200 and 1000 Hz. To ensure consistency throughout the experiment, several variables were kept constant:

(a) The distance between the sound level meter and the sound source was fixed at 10 cm.
(b) Each sample was tested for 30 seconds.
(c) The speaker volume was set to level 20 out of 100 for each pure tone. For safety, the use of headphones was recommended to prevent prolonged exposure to loud noise.

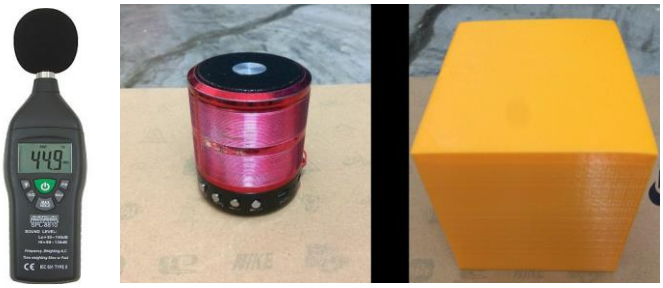

Figure 5. Sound Reductions Experimental Setup consists of Sound Level Meter, Wireless Speaker, and Acoustic Enclose Sample

To verify the accuracy of the experiment, each pure tone level was checked against its correct frequency before testing. The wooden acoustic enclosure was first placed over the speaker, and the sound level meter was activated simultaneously to record the equivalent SPL for 30 seconds. This procedure was then repeated for each acoustic enclosure sample. After testing at 200 Hz, the experiment was repeated sequentially for 300 Hz up to 1000 Hz to ensure comprehensive analysis.

3. Results and Discussions

This section discussed the results and findings obtained from the simulation of unit cell metamaterial design, acoustic enclosure samples fabrication and sound reduction experiment of different acoustic enclosures.

3.1 Simulation Result

The results of this simulation are applicable only to structures with rigid walls and hard boundaries. As illustrated in Figure 6, the acoustic pressure (AP) within the unit cell geometry is concentrated in the opening between the neck and cavity, supporting the mass-spring system theory in Helmholtz Resonators (HR). This opening serves as the air accumulation zone, where air from the neck area oscillates as it moves through the cavity volume. Meanwhile, the AP on the unit cell's surface is primarily concentrated along the cavity walls, demonstrating the oscillatory behavior of the structure as sound waves circulate within the area and gradually attenuate.

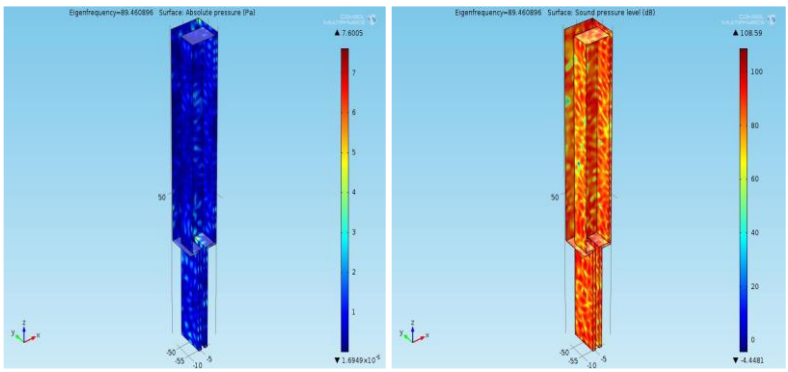

(a) (b)

Figure 6. AP on (a) Volume and (b) Surface of Unit Cell Geometry

The eigenfrequency for the volume of the unit cell was found to be 89.46 Hz, while for the surface of the unit cell, it was 90.12 Hz. These frequencies fall below the targeted frequency range for sound reduction, confirming that the structure and its parameters can interact with the desired sound waves without inducing vibrations.

To further validate the design, the sound pressure level (SPL) of the unit cell was analyzed to determine its resonant frequency, which was then compared with both calculated and experimental results. As shown in Figure 7, the highest SPL occurred at 773 Hz, indicating that sound waves with frequencies higher than 773 Hz can be effectively reduced by the unit cell, while lower frequencies remain unaffected.

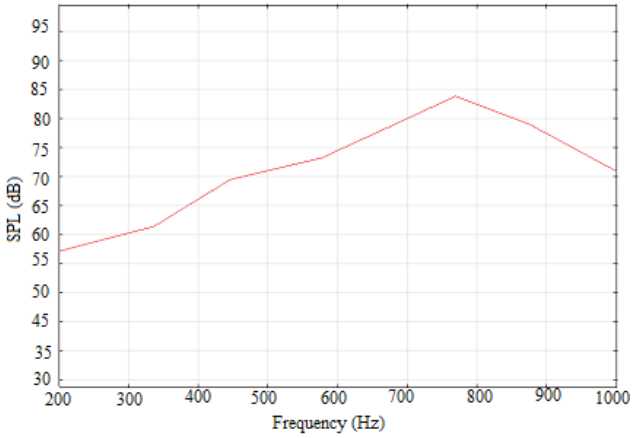

Figure 7. Graph of SPL versus Frequency

3.2 Comparison on Fabrication Process

The performance comparison of each acoustic enclosure sample in terms of fabrication process is presented in Table 2. Among all the samples, the wood acoustic enclosure posed the greatest fabrication challenge, as it required multiple manual tasks such as estimating, marking, cutting, smoothing, and assembling. Additionally, the reliance on manual measurement and estimation increased the likelihood of errors due to human factors, whereas 3D printing technology minimized such errors by relying on precise machine-based fabrication.

Regarding fabrication duration, digital fabrication generally took longer than manual fabrication. However, the preparation phase for digital fabrication, loading the file and setting up the printer, only required 10 to 15 minutes. The remaining time was dedicated to the printing process, which operated autonomously, allowing the user to multitask. In contrast, manual fabrication demanded constant attention and continuous handwork until completion. Additionally, 3D-printed samples were ready for testing immediately, whereas the wood samples required drying time for the acoustic sealant before they could be tested. Moreover, the printing process for metamaterial-based samples took longer due to the increased number of surfaces. ABS samples printed faster than PLA samples because ABS has a lower melting point, requiring less heating time for both the filament and the printer platform, thereby reducing the overall printing duration.

In terms of fabrication cost, PLA and ABS samples were the most cost-effective, as these materials are widely available in the market at affordable prices. The total fabrication cost for 3D-printed samples was limited to the filament usage, with a single spool of ABS or PLA filament costing around RM80.00, enough to produce all four 100 mm^3 acoustic enclosures from the same spool. On the other hand, the cost of fabricating wood samples was higher, as it included both the raw material and the acoustic sealant required for assembly.

Table 2. Fabrications of Acoustic Enclosure Samples

Sample	Fabrication method	Difficulties	Duration in hours (h) and minutes (min)	Cost (RM)
Wood	Manual handwork	Designing & developing	8 h	40.00
ABS	3D printing	Designing	24 h 12 min	20.00
PLA	3D printing	Designing	23 h 28 min	20.00
PLA Metamaterial (1mm)	3D printing	Designing	23 h37 min	20.00
PLA Metamaterial (5mm)	3D printing	Designing	23 h 54 min	20.00

3.3 Performance of Acoustic Enclosure

The performance of each acoustic enclosure sample in reducing sound was observed based on the SPL reading shown in Table 3. PLA with metamaterial of 5 mm thickness reduced all sound source from 200 Hz to 1000 Hz. PLA with metamaterial of 5 mm thickness is the best sound reducing material followed by PLA with metamaterial of 1 mm thickness, PLA, ABS, and wood. The lowest SPL recorded was 52.6 dB (in the range of acceptable limit) from PLA with metamaterial of 5 mm thickness during 800 Hz frequency.

Table 3. SPL of Different Acoustic Enclosure

	***f*, Hz**	**200**	**300**	**400**	**500**	**600**	**700**	**800**	**900**	**1000**
SPL (dB)	Source	59.4	72.3	76.2	76.2	76.7	76.0	78.7	78.6	78.6
	Wood	61.8	75.2	5.9	76.0	75.6	73.4	66.2	66.4	66.9
	ABS	61.2	74.8	75.2	75.2	73..7	73.0	66.2	61.5	65.9
	PLA	60.7	73.4	74.7	74.5	71.6	69.5	64.9	55.1	60.6
	PLA MM (1mm)	61.3	74.1	74.7	74.5	71.5	69.1	63.6	54.5	57.8
	PLA MM (5mm)	58.4	70.9	74.3	73.9	70.7	68.3	52.6	56.6	57.3

According to Table 4, the pattern of decibel drop (d) increased progressively from the wood sample to the PLA with metamaterial (5 mm thickness). The decibel drop (d) began at 400 Hz for the wood, ABS, PLA, and PLA with metamaterial (1 mm thickness) samples, whereas for PLA with metamaterial (5 mm thickness), it started at 200 Hz due to the presence of additional resonant cavities.

Based on the Helmholtz Resonator (HR) principle, increasing the thickness of unit cell structures leads to a larger cavity volume (Vcavity) in the resonance system, creating more space for sound attenuation. The four other samples exhibited an increase in SPL when exposed to frequencies between 200 and 300 Hz, indicating that greater thickness is required to effectively influence low frequencies and reduce SPL. For frequencies above 500 Hz, there was a notable reduction in d, as higher frequencies are easier to attenuate due to their shorter wavelengths.

The PLA with 5 mm metamaterial sample achieved its highest d at 800 Hz, whereas the other four samples peaked at 900 Hz. The PLA with metamaterial demonstrated the most effective sound reduction due to the presence of metamaterial structures and resonance effects. The incorporation of multiple resonant structures within the acoustic enclosure significantly reduced sound levels by more than 20 dB, bringing them to an acceptable SPL that is less harmful to human hearing.

Table 4. Decibel Drop of Different Acoustic Enclosures

	***f*, Hz**	**200**	**300**	**400**	**500**	**600**	**700**	**800**	**900**	**1000**
d, dB	Wood	-	-	0.3	0.2	1.1	2.6	12.5	16.2	11.7
	ABS	-	-	1.0	1.0	3.0	3.0	12.5	17.1	12.7
	PLA	-	-	1.5	1.7	5.1	6.5	13.8	23.5	18.0
	PLA MM (1mm)	-	-	1.5	1.7	5.2	6.9	15.1	24.1	20.8
	PLA MM (5mm)	1.0	1.4	1.9	2.3	6.0	7.7	26.1	22.0	21.3

The wood sample exhibited the lowest decibel drop (d) across the 400 to 1000 Hz frequency range due to the presence of uncertainties in air gaps between walls and the acoustic properties of the sealant, allowing sound waves to escape rather than being fully attenuated within the acoustic enclosure. Since air can pass through the material, it also enables sound transmission, reducing its overall effectiveness. In contrast, digital fabrication allowed for the creation of a single, solid structure, minimizing potential air gaps and enhancing sound attenuation performance.

Traditional noise barrier technology requires at least a 3×3 meter concrete wall to achieve a 20 dB reduction in sound. However, the same level of sound attenuation can be achieved using PLA with 5 mm metamaterial. As shown in Table 5, the cost of constructing an acoustic metamaterial is less than half of the cost of building conventional noise barriers. This suggests that acoustic metamaterials have the potential to replace traditional materials in noise barrier applications, offering effective sound reduction at a significantly lower development cost.

Table 5. Developments Costing of Noise Barrier

Material	**Unit**	**Price per unit**	**Price per meter sq**
Concrete	1x1 m	800-1000	800-1000
Metamaterial	100x100 mm	10-20	100-200

4. Conclusion

In this study, the PLA acoustic enclosure with a 5 mm thick metamaterial demonstrated the highest sound reduction capability among all tested samples, achieving a maximum sound pressure level reduction of 26.1 dB at 800 Hz. The successful development of an acoustic enclosure with metamaterial for noise control applications was achieved, highlighting its effectiveness in sound attenuation. Additionally, the use of 3D printing technology significantly improved the fabrication process, reducing both time and cost. The findings also indicate that a PLA acoustic enclosure with a 5 mm metamaterial thickness outperformed its 1 mm counterpart in sound reduction, confirming that greater metamaterial thickness enhances sound attenuation performance.

This study can be further refined by exploring variations in dimensions, the number of Helmholtz resonators, and their arrangement within the acoustic enclosure. Future research should also focus on analyzing different unit cell metamaterial patterns and their impact on sound reduction.

Additionally, the liquid/gas two-phase flow interface and its void fraction were experimentally analyzed using a conductive wire-mesh tomography sensor. A circular wire-mesh sensor was specifically designed for a circular cross-sectional test section of 7178.0366 mm². The wire-mesh tomography technique proved to be a reliable method for measuring the liquid/gas two-phase flow interface and void fraction. However, to achieve greater accuracy in estimating the gas-liquid interface, further advancements in algorithm development are required.

Acknowledgment

The author would like to thank Universiti Teknologi Malaysia (UTM) for providing facilities for this study.

References

[1] Luxon, L. M., & Prasher, D, *Noise and its effects*. Wiley, 2007.
[2] Wise, S., & Leventhall, G., "Active noise control as a solution to low frequency noise problems. Low Frequency Noise", *Vibration and Active Control*, 29(2), 129-138, 2010.
[3] Guenneau, S., & Craster, R. V., "Fundamentals of Acoustic Metamaterials", *Acoustic Metamaterials Springer Series in Materials Science*. 1-42, 2013.
[4] Wang, Q. "Studies On The Relationship Between Sound Absorption", *Acta Polymerica Sinica*, 008(6), 517-521, 2008.
[5] Takahashi, Y., "Vibratory sensation induced by low-frequency noise: A pilot study on the threshold level. Low Frequency Noise", *Vibration and Active Control*, 28(4), 245-253, 2009.
[6] Simon, F., "Low frequency sound absorption of resonators with flexible tubes", *The Journal of the Acoustical Society of America*, 133(5), 3265, 2013.
[7] Sanchez-Dehesa, J., Chocano, V. M., & Guild, M. D., "Recent results on sonic crystals for sound guiding and acoustic absorption", *The Journal of the Acoustical Society of America*, 136(4), 2076-2076, 2014.
[8] Zhang, S. (2010). *Acoustic metamaterial design and applications*. Unpublished doctoral dissertation, University of Illinois.
[9] Active Standard ASTM C423, *Standard Test method for sound absorption and sound absorption coefficients by the reverberation room method*. ASTM International,West Conshocken, PA, 2017.
[10] Herrero-Durá, I., Picó, R., Sánchez-Morcillo, V., Garcia-Raffi, L. M., & Romero-García, V. "Vibroacoustic effects of resonant sonic crystals in sound absorption", *European Acoustics Association Journal*, 2015.
[11] Mast, T. Dougles., *Helmholtz resonator*. AccessScience. McGraw-Hill Education, 2014.
[12] Liang, Z., Feng, T., Lok, S., Liu, F., Ng, K. B., Chan, C. H., Li, J., "Space-coiling metamaterials with double negativity and conical dipersion", *Scientific Reports*, 3, 1614, 2013.
[13] Jiménez, N., Huang, W., Romero-García, V., Pagneux, V., & Groby, J. P., "Ultra-thin metamaterial for perfect and quasi-omnidirectional sound absorption", *Applied Physics Letters*, (109), 121902nd, 2016.
[14] Sandberg U. Plenary paper published in *the Proceedings of the 2001 International Congress and Exhibition on Noise Control Engineering*, Hague, Netherlands, 2001.
[15] Sood, D., & Tripathi, C. C., "A Wideband Wide-Angle Ultra-Thin Metamaterial Microwave Absorber", *Progress In Electromagnetics Research* M, 44, 39-46, 2015.
[16] Claeys, C. C., Pluymers, B. & Desmet, W., "Design of a resonant metamaterial based acoustic enclosure Leuven", *Flanders*, 3351-3358, 2014.
[17] Araque, J. L., & Baena, J. D. , "Duality for 3D metamaterial resonators", *International Congress on Advanced Electromagnetic Materials in Microwaves and Optics*, 2014